Journal of Crystal Growth 312 (2010) 2861–2864

Contents lists available at ScienceDirect

Journal of Crystal Growth

journal homepage: www.elsevier.com/locate/jcrysgro

A route to single-crystalline ZnO films with low residual electron concentration

J.S. Liu [a,b], C.X. Shan [a,*], S.P. Wang [a,b], F. Sun [a,b], B. Yao [a], D.Z. Shen [a]

[a] Key Laboratory of Excited State Processes, Changchun Institute of Optics, Fine Mechanics and Physics, Chinese Academy of Sciences, Changchun 130033, China
[b] Graduate School of Chinese Academy of Sciences, Beijing 100049, China

ARTICLE INFO

Article history:
Received 14 May 2010
Accepted 5 July 2010
Communicated by D.P. Norton
Available online 13 July 2010

Keywords:
A1. X-ray diffraction
A3. Molecular beam epitaxy
B1. Zinc compounds
B2. Semiconducting II–VI materials

ABSTRACT

Single-crystalline ZnO films have been grown on *a*-plane sapphire in plasma assisted molecular beam epitaxy by introducing a high-temperature ZnO buffer layer. The residual electron concentration of the films can be lowered to 1.5×10^{16} cm^{-3}, comparable with the best value ever reported for ZnO films grown on a rare and costly substrate of $ScAlMgO_4$. A 3×3 reconstruction has been observed on the films grown in this route, which reveals that the films have very smooth surface. X-ray phi-scan spectrum of the films shows six peaks with 60° intervals, and two-dimensional X-ray diffraction datum indicates the single-crystalline nature of the films. Low temperature photoluminescence spectrum of the films shows a dominant free exciton emission and five phonon replicas, confirming the high quality of the films.

1. Introduction

Zinc oxide (ZnO) has recently been a potential candidate for the applications in short-wavelength optoelectronic devices such as light-emitting diodes (LEDs) and laser diodes (LDs) for its large band gap of 3.37 eV and large exciton binding energy of 60 meV [1–3]. However, the aforementioned applications are drastically hindered by the difficulties in realizing reliable and reproducible p-type ZnO [4]. It is accepted that the difficulties are mainly caused by the strong compensation arising from the high residual electron concentration [5–11]. Therefore, obtaining high quality ZnO films with relatively low residual electron concentration is a fundamental step towards efficient p-type doping and future applications in optoelectronic devices of ZnO. The lowest residual electron concentration ever reported in ZnO films is 1×10^{16} cm^{-3}, which was realized in ZnO films grown on lattice-matched $ScAlMgO_4$ (SCAM) substrates [12]. Nevertheless, the SCAM substrate is rare and costly, and is still not commercially available. Therefore obtaining high quality ZnO films with relatively low residual electron concentration on common substrate, such as sapphire, is of great importance and significance. Although quite a few reports have demonstrated the realization of high quality ZnO films on sapphire [13–17], a systematic route to high quality ZnO films with low electron concentration is still lacking and eagerly wanted.

In this paper, a route to high quality ZnO films with low electron concentration has been proposed and confirmed. The residual electron concentration in the films grown on a common sapphire substrate can be lowered to about 1.5×10^{16} cm^{-3} in this method, comparable with the best value reported by Tsukazaki et al. [12] on SCAM substrate.

2. Experiment

The ZnO thin films studied in this paper were grown by VG-V80H plasma-assisted molecular beam epitaxy (MBE); a-plane sapphire has been employed as substrate for the growth. It has been demonstrated that *a*-plane sapphire is helpful in reducing the residual electron concentration of the ZnO films in our previous paper. The sapphire substrate was cleaned in an ultrasonic bath in acetone for 10 min and ethanol for 5 min, followed by de-ionized water rinsing for 5 min. Then the substrate was etched in a mixed solution of H_2SO_4:H_3PO_4=3:1 at 160 °C for 15 min. Finally the substrate was washed with de-ionized water and blown dried using nitrogen gas. After chemical cleaning and etching, the substrate was heated at about 600 °C for 30 min in a preparation chamber to remove possible adsorbed surface contamination. Then it was sent into the growth chamber. 6 N-purity zinc held in a Knudsen effusion cell and 5 N-purity O_2 activated in an Oxford Applied Research Model HD25 radio-frequency (13.56 MHz) plasma source were employed as precursors for the growth of ZnO films. Before growth, the substrate was treated by oxygen plasma at 800 °C for 15 min to provide an oxygen-terminated surface [13]. During the growth process, the

* Corresponding author. Tel./fax: +86 43186176298.
E-mail address: phycxshan@yahoo.com.cn (C.X. Shan).

0022-0248/$ - see front matter © 2010 Elsevier B.V. All rights reserved.
doi:10.1016/j.jcrysgro.2010.07.006

pressure in the growth chamber was fixed at 1×10^{-5} mbar. The growth was initiated by depositing a thin ZnO layer at 850 °C for 20 min, then the substrate temperature was fixed at 800 °C for another 3 h, and ZnO films were also grown on *a*-plane sapphire under the same conditions except that no such high temperature layers were introduced for comparison.

The growth process was monitored by *in-situ* reflection high energy electron diffraction (RHEED). Electrical properties of the films were measured in a Hall measurement system (Lakeshore 7707) under Van der Pauw configuration. Crystal structure of the films was studied with Bruker D8 GADDS X-ray diffraction using CuKα ($\lambda = 1.54$ Å) as the excitation source. Surface morphology of the films was characterized in a field-emission scanning electron microscope (Hitachi S-4800). Photoluminescence (PL) measurements of the films were carried out by employing the 325 nm line of a He–Cd laser as the excitation source.

3. Results and discussion

The surface morphologies of the ZnO films with and without the high temperature layer are displayed in the SEM images as shown in Fig. 1. The ZnO film grown on sapphire without the high temperature layer exhibits a uniform texture surface with some crystallites on it (Fig. 1(a)), while the ZnO film with the high temperature layer shows a much smoother surface (Fig. 1(b)). To investigate the effect of the high temperature buffer layer, the SEM image of the buffer layer is shown in Fig. 1(c). The surface morphology of this layer exhibits a pattern close to the one shown in Fig. 1(b), from which one can deduce that the high temperature buffer layer may play a template role for the subsequent growth of the ZnO films.

The electrical properties of the films are listed in Table 1. Hall mobility of the ZnO film with the high temperature buffer layer is similar to that of the film without the buffer layer, but the residual carrier concentration is as low as 1.5×10^{16} cm^{-3}, which is about one order of magnitude lower than that of the latter (2×10^{18} cm^{-3}). It is noteworthy that the value is comparable to the lowest residual electron concentration ever reported in ZnO films grown on SCAM, which is 1×10^{16} cm^{-3} [12]. Also we note that the decreased residual electron in the ZnO films with high temperature buffer layer is not occasional; tens of growths have been carried out and the same trend has been obtained. It is thought that the introduced buffer layer will serve as a high quality template that avoids the strain caused by the lattice and thermal mismatch between ZnO films and sapphire; as a result, electron concentration of the ZnO films is reduced.

In order to eliminate the effect of the lattice and thermal mismatch between the ZnO layer and sapphire substrate further, a 500 nm ZnO film deposited on sapphire substrate was employed as the starting points of growth. In this case, the ZnO/sapphire acts as a homoepitaxial substrate. The SEM image and RHEED pattern of the ZnO film grown on the ZnO/sapphire template are shown in Fig. 2. The SEM image shows a mirror-like surface without any crystallites. The RHEED pattern also shows bright streaks; a 3×3 reconstruction can also be observed, as shown in Fig. 2(b), which reveals that the film we obtained has a smooth surface.

Fig. 3 shows the structural characterizations of the ZnO film with the high temperature buffer layer grown on ZnO/sapphire substrates. In XRD θ–2θ pattern, as shown in Fig. 3(a), besides the diffraction from the sapphire substrate, only one peak can be observed and the peak can be indexed to the diffraction from (0 0 0 2) facet of wurtzite ZnO. The strong (0 0 0 2) diffraction peak indicates that the ZnO film is crystallized in wurtzite structure with a *c*-axis preferred orientation. XRD phi-scan

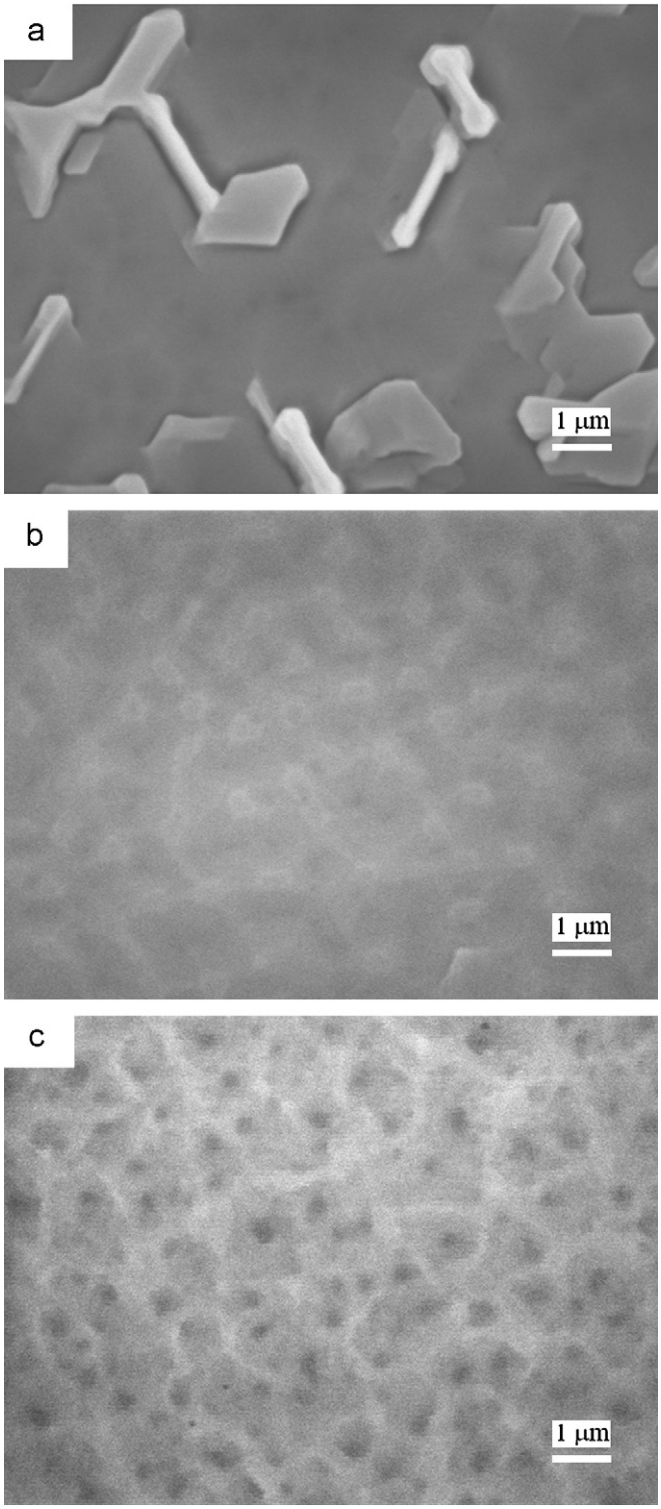

Fig. 1. SEM images of the ZnO films without (a) and with (b) the high temperature buffer layer grown on sapphire substrates and (c) the SEM image of the high temperature ZnO buffer layer.

Table 1
Hall data of the ZnO films grown on sapphire substrate with and without the high temperature buffer layer.

Sample	Hall mobility (cm^2/V s)	Carrier concentration (cm^{-3})
Without buffer	22	2.0×10^{18}
With buffer	28	1.5×10^{16}

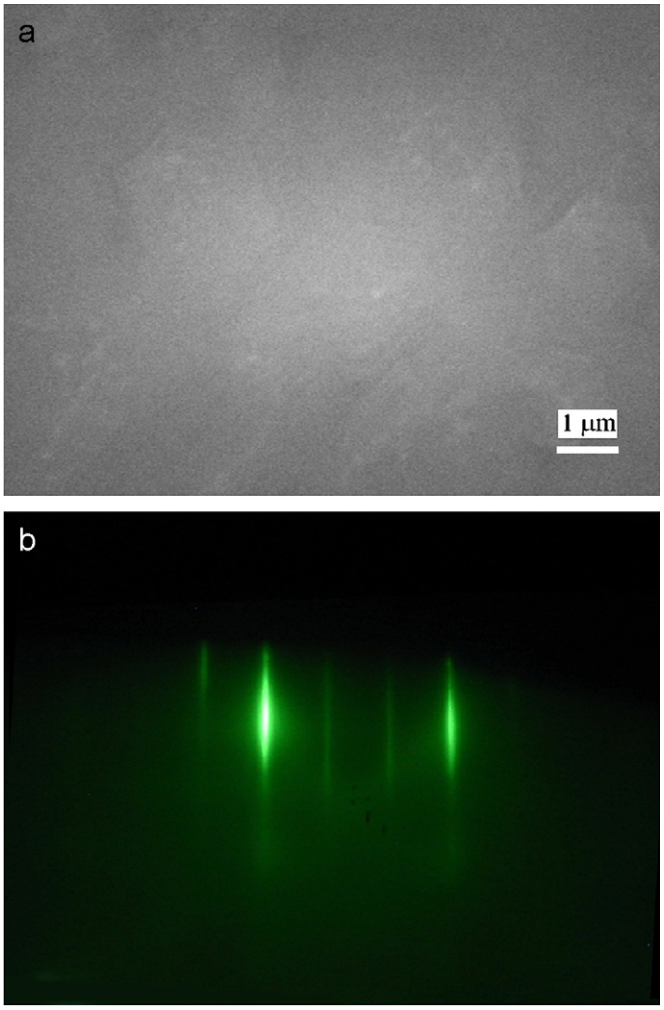

Fig. 2. SEM images (a) and RHEED pattern (b) of ZnO films with the high temperature layer grown on ZnO/Al_2O_3 substrates.

analysis is very effective in identifying the in-plane orientation. Six well-defined peaks with 60° interval in the pattern are clearly seen, which indicates the film has a 6-fold symmetry, as shown in Fig. 3(b). Two-dimensional XRD (2D-XRD) is also used to explore the in-plane atom arrangement of the sample. An ideal 2D-XRD image for a single crystalline film is a focused point. One full diffraction ring in the 2D-XRD symbolizes the random arrangement of the in-plane atoms in the film. As can be seen in Fig. 3(c), the image of the film gives two focused points (one is for sapphire, the other is for ZnO film), which reveals the uniform in-plane atom arrangement and structure textural isotropy of the film.

Low temperature photoluminescence spectrum was also employed to investigate the optical quality of the films. Fig. 4 shows the PL spectra of the ZnO films measured at 70 K. A dominant peak can be observed at 3.377 eV, which can be attributed to the free exciton of ZnO [18,19]. At the lower energy side, the peak at 3.365 eV can be ascribed to the exciton bounded to neutral donors [20]. Five peaks at 3.314, 3.242, 3.170, 3.098 and 3.027 eV can also be observed in the spectrum, which can be attributed to the longitudinal optical (LO) phonon replicas of free excitons [21]. This is the first report of five phonon replicas of the free exciton in ZnO films to our knowledge. The dominant free exciton emission and appearance of up to five phonon replicas of the free exciton emission confirm the relatively high quality of the ZnO films.

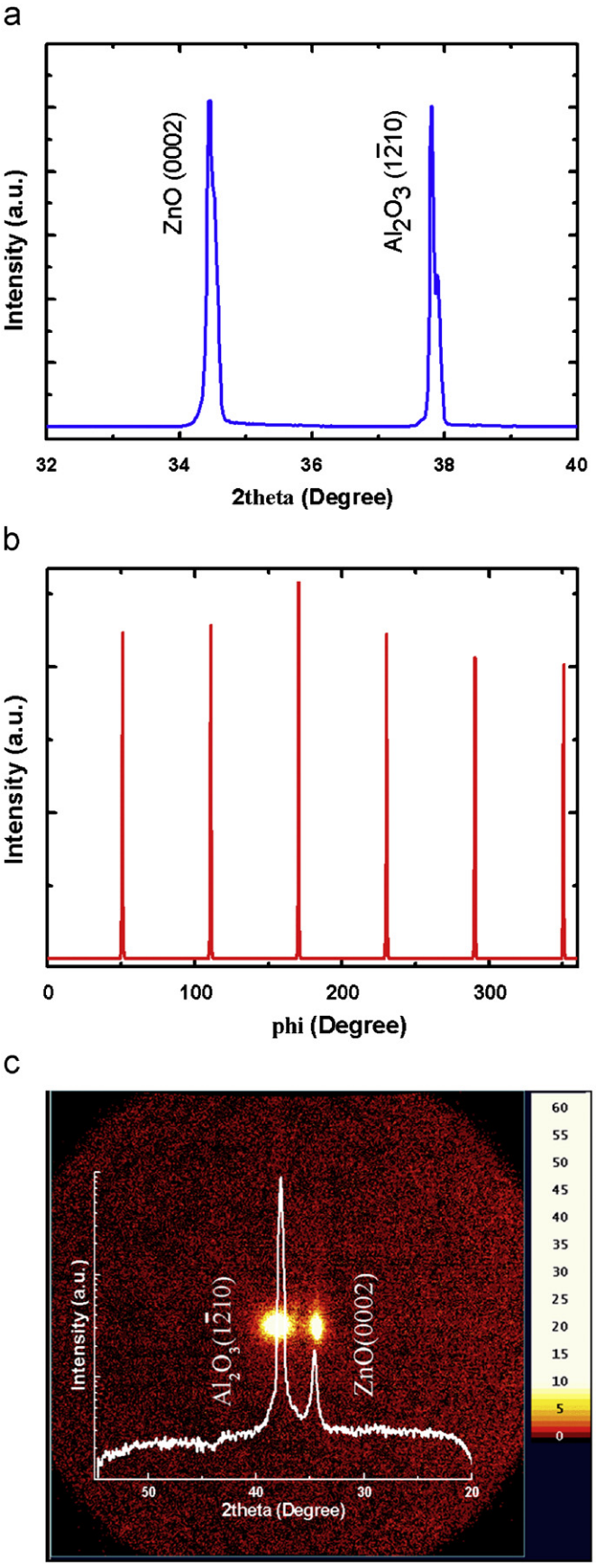

Fig. 3. θ–2θ XRD spectrum (a), XRD phi-scan pattern (b) and 2D-XRD image (c) of the ZnO films with high temperature buffer layer grown on ZnO/Al_2O_3 substrates.

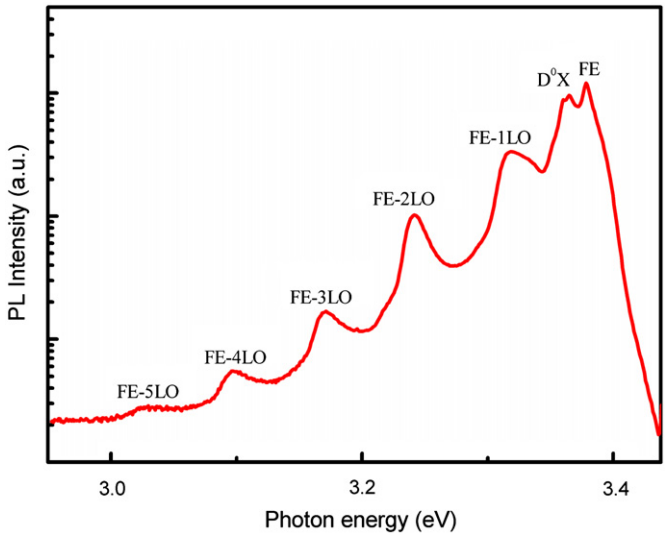

Fig. 4. 70 K PL spectrum of the ZnO films with high temperature buffer layer grown on ZnO/Al_2O_3 substrates.

4. Conclusion

In summary, high quality ZnO films with a low carrier concentration have been obtained by introducing a thin high-temperature ZnO buffer layer. The buffer layer facilitates the initial nucleation and promotes the subsequent growth of ZnO film, thus resulting in a smooth surface morphology, especially on the ZnO/sapphire substrates. The value of the residual carrier concentration is $1.5 \times 10^{16}\ cm^{-3}$, which is comparable to the best value ever reported in ZnO films grown on a rare and costly substrate of SCAM. The results reported in this paper may provide a promising route to high quality ZnO films on common sapphire substrates with low residual electron concentration and thus lay a solid ground for the future p-type doping and applications of ZnO in optoelectronic devices.

Acknowledgements

This work was supported by the Knowledge Innovation Program of the CAS (KJCX3.SYW.W01), the "973" program (2006CB604906), the Natural Science Foundation of China (10774132, 60776011, 10974197 and 60976040), and The Instrument Developing Project of Chinese Academy of Sciences (YZ200903).

References

[1] D.M. Bagnall, Y.F. Chen, Z. Zhu, T. Yao, S. Koyama, M.Y. Shen, T. Goto, Appl. Phys. Lett. 70 (1997) 2230.
[2] Z.K. Tang, G.K.L. Wong, P. Yu, M. Kawasaki, A. Ohtomo, H. Koinuma, Y. Segawa, Appl. Phys. Lett. 72 (1998) 3270.
[3] D.C. Look, Mater. Sci. Eng. B 80 (2001) 383.
[4] S.B. Zhang, S.H. Wei, A. Zunger, J. Appl. Phys. 83 (1998) 3192.
[5] D.C. Look, B. Claflin, Phys. Status Solidi B 241 (2004) 624.
[6] S.B. Zhang, S.H. Wei, A. Zunger, Phys. Rev. B 63 (2001) 075205.
[7] A. Kobayashi, O.F. Sankey, J.D. Dow, Phys. Rev. B 38 (1983) 946.
[8] C.G. Van de Walle, Phys. Rev. Lett. 85 (2000) 1012.
[9] A.F. Kohan, G. Ceder, D. Morgan, C.G. Van de Walle, Phys. Rev. B 61 (2000) 15019.
[10] D.C. Look, C. Coskun, B. Claflin, G.C. Farlow, Physica B 340–342 (2003) 32.
[11] D.C. Look, J.W. Hemsky, J.R. Sizelove, Phys. Rev. Lett. 82 (1999) 2552.
[12] A. Tsukazaki, T. Onuma, M. Ohtani, T. Makino, M. Sumiya, K. Ohtani, S.F. Chichibu, S. Fuke, Y. Segawa, H. Ohno, H. Koinuma, M. Kawasaki, Nat. Mater. 4 (2005) 42.
[13] Y.F. Chen, D.M. Bagnall, H.J. Koh, K.T. Park, K. Hiraga, Z.Q. Zhu, T. Yao, J. Appl. Phys. 84 (1998) 3912.
[14] Y.F. Chen, H.J. Ko, S.K. Hong, T. Yao, Appl. Phys. Lett. 76 (2000) 559.
[15] Y.R. Ryu, T.S. Lee, H.W. White, J. Cryst. Growth 261 (2004) 502.
[16] K. Hirano, M. Fujita, M. Sasajima, T. Kosaka, Y. Horikoshi, J. Cryst. Growth 301–302 (2007) 370.
[17] S.K. Hong, H.J. Ko, Y.F. Chen, T. Yao, J. Cryst. Growth 209 (2000) 537.
[18] D.C. Reynolds, D.C. Look, B. Jogai, Phys. Rev. B 60 (1999) 2340.
[19] C.X. Shan, Z. Liu, S.K. Hark, Appl. Phys. Lett. 92 (2008) 073103.
[20] H.J. Ko, Y.F. Chen, T. Yao, K. Miyajima, A. Yamamoto, T. Goto, Appl. Phys. Lett. 77 (2000) 537.
[21] F.Y. Jiang, J.N. Dai, L. Wang, W.Q. Fang, Y. Pu, Q.M. Wang, Z.K. Tang, J. Lumin. 122 (2007) 162.